ASIA TURBOMACHINERY & PUMP SYMPOSIUM
12-15 MARCH 2018
SUNTEC SINGAPORE

Design and Implementation of Swirl Brakes for Enhanced Rotordynamic Stability in an Off-shore Centrifugal Compressor

Balaji Venkataraman,
David Moulton, Mike Cave,
Chris Clarke,
Solar Turbines Inc.,
San Diego, CA, USA

Jason Wilkes, Jeff Moore
Southwest Research Institute,
San Antonio, TX, USA

Thom Eldridge
Shell Americas, Upstream,
Houston, TX, USA

Balaji Venkataraman is the Manager of Rotordynamics, Gas Compressor Products at Solar Turbines, Inc.. He has been with Solar for over 19 years. His group is responsible for rotordynamic designs, testing, field reliability and product quality of compressors from vibration standpoint. Balaji has extensive experience in vibrations, trouble-shooting and resolution of vibration issues, seal design and damper bearings. Prior to joining Solar, Balaji had worked with Atlas Copco and had been a visiting researcher at NASA's Marshall Space Flight Center, Huntsville, AL. Balaji holds a Master's degree from Texas A&M University.

David Moulton is an electromechanical engineer with 29 years of turbomachinery experience. He received a B.S. in Engineering from University of California, Irvine in 1988. His simple career began, and continues, with Solar Turbines Inc. in San Diego, California. In the Gas Compressor Engineering group, roles have included structural analysis, project management, conceptual design, resolution of test and field issues, and analysis of floating ring oil seals and semi-abradable labyrinth seals. David's interests include application of electric motors to centrifugal compressors.

Michael Cave is the Manager for gas compressor aerodynamics and performance for Solar Turbines, Inc., a division of Caterpillar. Mike started his career with Solar in 1994 as a Senior Design engineer in gas compressors and becoming manager in 1997. Mike graduated with a BS in Mechanical Engineering for The Ohio State University. Prior to joining Solar, Mike worked for Honeywell Propulsion Systems in Phoenix, Arizona. There he was an aero engineer for both axial and centrifugal compressors used for aircraft propulsion systems.

Chris Clarke is a Senior Engineer in the Aerodynamics Performance and Design Group at Solar Turbines. He holds a PhD in Mechanical Engineering from Michigan State University and joined Solar in 2017. His previous work has focused on centrifugal gas compressor instability. His current work revolves around CFD applications to rotordynamic stability and the performance effects of compressor inlet geometry.

Dr. Jason Wilkes is a Senior Research Engineer in the Rotating Machinery Dynamics Section at Southwest Research Institute in San Antonio, TX. His experience at SwRI includes design and construction of various test rigs, predicting lateral and torsional rotordynamic analyses, bearings and seals, and auxiliary bearing dynamics following failure of AMB supported turbomachinery. Dr. Wilkes holds a B.S., M.S., and Ph.D. in Mechanical Engineering from Texas A&M University where he worked at the Turbomachinery Laboratory for 6 years

Dr. Jeffrey Moore is an Institute Engineer within the Machinery Program at Southwest Research Institute in San Antonio, TX. He holds a B.S., M.S., and Ph.D. in Mechanical Engineering from Texas A&M University. His professional experience over the last 27 years includes engineering and management responsibilities related to centrifugal compressors and gas turbines at Solar Turbines Inc. in San Diego, CA, Dresser-Rand in Olean, NY, and Southwest Research Institute in San Antonio, TX. He has authored over 40 technical papers related to turbomachinery and is a member of the Turbomachinery Symposium Advisory Committee.

Thom Eldridge is Principle Technical Expert (PTE) of Rotating Equipment-Novel Technology for Royal Dutch Shell. He has participated in the off-shore Commissioning of a 900 bar injection compressor, as well as a 1000 bar Subsea Pump. Prior to this, Thom worked for Dresser-Rand as Supervisor of Rotordynamics and Manager of Aerodynamics. He served as Chairman of the 2009 ASME Gas Turbine User Symposium and has been a Session Chair for ASME IGTI from 2006-2010. He has contributed to API684 and API617 updates, presented numerous papers and short courses and holds two US patents. Thom graduated from Washington State University with BS and MS in Mechanical Engineering, and then from University of Nevada with an MBA. He has been a Registered Professional Engineer (State of California).

ABSTRACT

Rotordynamic stability of gas compressors at high speeds and operating pressures is a significant technical challenge. Dynamic instability must be avoided for the sake of safe, reliable and continuous operation of turbomachinery. Experience and literature have shown that one of the main sources of instability is the swirl within the secondary leakage path in shrouded impellers, especially the swirl entering the shroud seals. The technical brief presents the design and implementation of swirl brakes for centrifugal compressors with Teeth-on-Rotor seal configurations for shrouded impellers. Discussion includes (a) aerodynamic design of swirl brakes with the help of Computational Fluid Dynamics (CFD), (b) sub-scale testing of the swirl brake design in an instrumented single-stage test rig to measure the inlet swirl ratio in a shrouded impeller, (c) full-scale prototype shop-testing and qualification, with and without the swirl brakes in a closed-loop test facility, and (d) results of incorporating the swirl brakes at an off-shore compressor installation to improve rotordynamic stability.

INTRODUCTION

Rotordynamic stability of turbomachinery has been studied extensively during the past few decades. Literature (Benckert and Wachter, 1980 and Sivo et al. 1995) have shown that one of the main sources of rotordynamic instability in pumps is the swirl through the secondary leakage path in shrouded impellers, especially swirl entering the shroud seals. The same has been shown for centrifugal compressors by Baumann et al. (1999). Other features routinely employed by the industry for improving rotor stability include shunt-injection (Fozi, 1980) and hole-pattern seals (Moore, 2002).

Flow leaving the impeller tip enters the cavity between the stator and impeller shroud at high swirl velocities. The swirl velocity increases as the flow reaches the inlet to the shroud-seal on the impeller shroud. This in turn has been shown to generate significant tangential, destabilizing forces that can be detrimental to the overall rotordyamic stability of the compressor. In conjunction with the seals, the forces generated by the shroud cavity itself can be equally destabilizing. Predictions of shroud forces have been reported extensively by Childs (1993) and Moore and Palazzolo (1999). Minimizing the swirl ratio at the seal inlet (ratio of the fluid's circumferential velocity to rotor tip speed at the seal) is the goal of the swirl-brake design.

Nielsen (1998) performed analysis of swirl-brakes using 3D-Navier Stokes equations leading to more work on using CFD simulations of the swirl-brakes. Moore (2000) used a full viscous 3D model in CFD to design a swirl-brake and showed the possibility of creating a negative swirl within the vanes, thereby increasing compressor stability. More recently, Baldassarre et al. (2014) presented a methodology to optimize the design of swirl-brakes using CFD by analyzing the key attributes that impact its effectiveness. Untariou et al. (2013) used CFD to predict inlet swirl ratios to a balance drum seal in a centrifugal pump that shows instability without swirl-slots and a stable rotor with swirl-slots. Pugachev and Deckner (2012) compared experimental leakage and dynamic stiffness coefficients to CFD-based analytical results for a 3-stage brush seal.

It must be mentioned that while the industry has successfully used swirl-brakes for a few decades, many of these applications are for a Teeth-on-Stator configuration (TOS). Due to large wetted areas and practicality for assembly, developing an effective swirl-brake for Teeth-on-Rotor (TOR) has additional considerations. This paper presents the design, testing and successful implementation of swirl-brakes for a Teeth-on-Rotor configuration.

COMPRESSOR AND ROTOR DESIGN

Figure 1 shows the high-pressure compressor on which the swirl-brakes are implemented. The in-line compressor is pre-engineered, barrel-type, two-flange, with dry-gas seals or optional oil-seals. The Maximum Allowable Working Pressure of the compressor family ranges from 2250 to 4500 psia (155 to 300 bar). Several hundred units of this model are successfully operating in a world-wide fleet.

Figure 1. Compressor model at a site installation and driven by a gas turbine engine

Figure 2 depicts a typical modular-rotor, built-up with stub-shafts and impellers held together with a tie-bolt. The rotor chosen for the swirl-brake development is capable of accommodating up to 10-stages. Table 1 details key dimensions and attributes of the compressor/rotor-bearing system:

Figure 2. Modular rotor of the compressor

Table 1. Compressor and Rotor details

Parameters	Details	
Maximum Speed	22,300 rpm	
Slenderness ratio (Bearing span/Hub diameter)	10.5	
Bearings	5-pad tilt pad	
Bearing diameter	2.25”	57.1 mm
Max Allowable Working Pressure	2250 psia	155 bar
Impeller diameter	7.5”	190 mm

Prior full-scale stability testing on this 10-stage compressor had revealed the excitation of resonant sub-synchronous vibration (RSSV) at high speed when operating pressures exceeded 1600 psi (110 bar). Although the amplitude of the RSSV was bounded, the excitation of the resonant frequency was still unacceptable to the OEM. Consequently, applications for

new sales were limited near the known stability threshold. But changes in operating conditions at a few existing installations of this compressor model led the end-users and the OEM to consider alternatives to improve the stability threshold. Many options were considered, but any significant modification to the existing pre-engineered rotor design was ruled out due to commercial and logistical reasons. Implementing swirl brakes was determined to be the most effective option.

DESIGN OF THE SWIRL-BRAKE USING CFD

The aerodynamic forces inside a centrifugal compressor stage shroud cavity can induce destabilizing rotordynamic cross-coupling forces. These forces are caused by secondary leakage flows in the shroud cavity and are tied to the swirl within the cavity and the seals. Eliminating or minimizing the swirl leads to a significant decrease in cross-coupled force, thereby improving the rotordynamic stability (Sivo, 1995 and Baumann, 1999).

In the study hereby presented, the goal was to develop a satisfactory swirl-brake design that (a) would limit the swirl developed in the cavity and upstream of the seal, thereby improving rotordynamic stability, (b) have a minimal effect on the overall stage aerodynamic performance, and (c) be easy to implement without any major component modifications in the pre-engineered compressor. One key aspect of the compressor is that the shroud-seals and hub-seals are of the Teeth-on-Rotor (TOR) type. The labyrinth sealing teeth are machined on the impeller's shroud and hub locations. The stators are fitted with abradable seal rings on which the rotating teeth seals the secondary leakage flow (from impeller discharge to the suction). Figure 3 shows the seal ring (baseline) and two swirl-brake configurations.

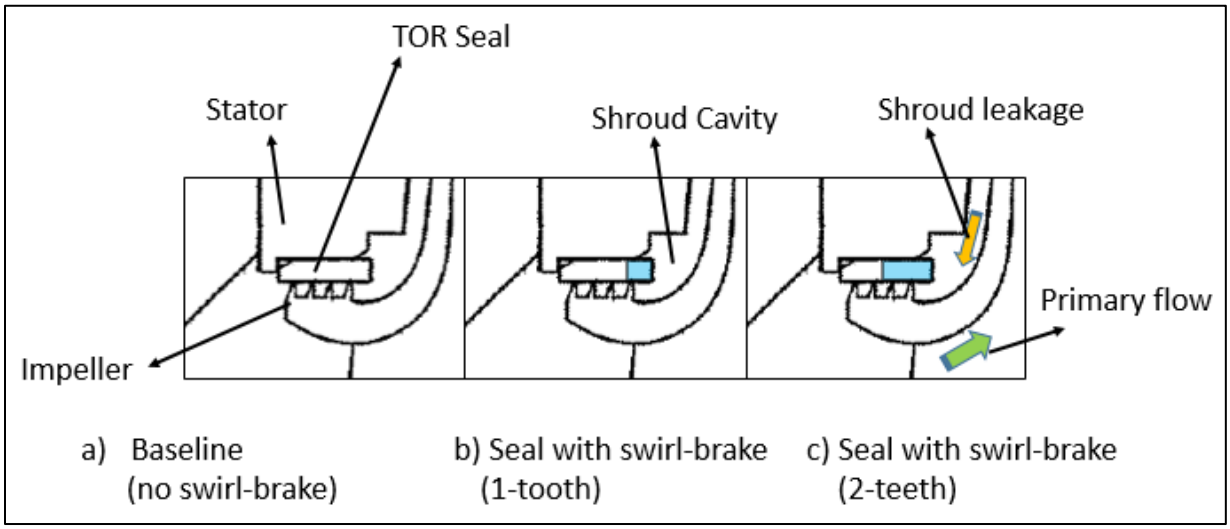

Figure 3. Schematic views of baseline, TOR seal and configurations with swirl-brakes.

There is extensive literature (as referenced earlier) on swirl-brakes for Teeth-on-Stator (TOS) type seals, based on their wide prevalence in many compressor applications. However, not much has been reported on TOR seals with swirl-brakes for compressors. The swirl-brakes for TOR types are essentially seal rings with several slots milled around the circumference, right at the entrance to the seal (or the first labyrinth tooth). The slots act as a "reservoir" to trap the

leakage flow, with the geometry sized to create free vortices that reduce the swirl just upstream of the first sealing tooth. This also impacts the swirl upstream in the shroud cavity.

Due to the fluid flow path and the need to maintain a minimum axial distance between the edge of the seal and the impeller shroud to avoid rubs, it was not possible to extend the seal axial length. Hence, the swirl-brake seal design allowed for the loss of one or two sealing teeth, as depicted in Figure 3. This methodology provided the option to either use seal rings without the swirl-brakes or with the swirl-brakes, ensuring easy inter-changeability of parts. No other components were modified. It was anticipated that the use of swirl brakes would increase the stage leakage flow due to the loss of sealing teeth, so an optimization of geometry was performed between the seal rotordynamic attributes and the stage aerodynamic performance.

Figure 4 shows a typical swirl-brake with key dimensions for a Teeth-on-Rotor configuration. A few different configurations of the swirl brakes were studied, with a varying number of slots and geometry. The key parameters optimized were (a) Chord length of the slot, (b) # of slots, and (c) Pitch-to-Chord ratio. All optimization was performed through modeling and simulation of the various configurations with the help of Computational Fluid Dynamics (CFD).

A fully developed geometry was used to create the volume mesh, see Figures 5 and 6, for simulation, setup, run, and post-processing the results. For this study, it was found that a pie slice model incorporating one swirl-brake passage and the corresponding cavity flow path was sufficient for simulation. The secondary leakage path mesh had roughly 372,000 nodes and 1 million elements. Including the impeller primary passage, the full geometry contained 750,000 nodes and 1.5 million elements. The simulation employed the k-ϵ turbulence model. The overall y+ from the simulations in the seal region was below 10.

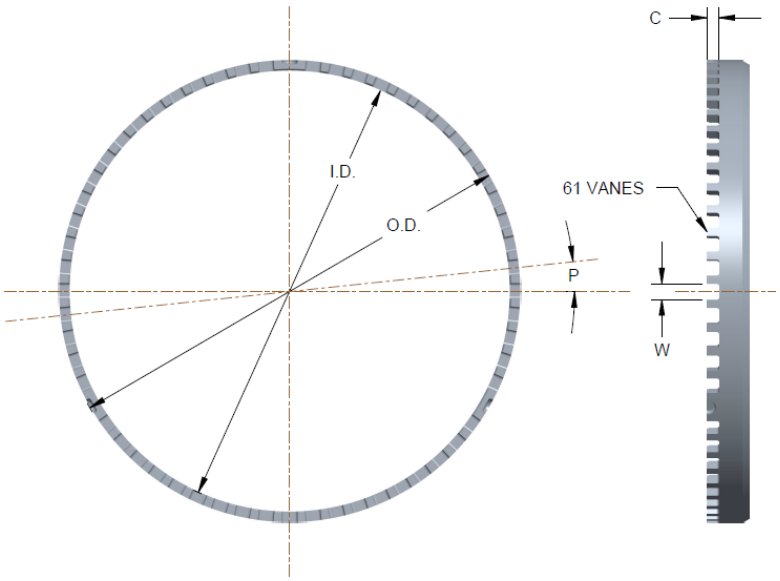

Nomenclature

ID, OD : Labyrinth Seal diameters (inside and outside, respectively)
P: Total Pitch of the swirl-slots, includes wall thickness
W: Pitch of the swirl-slots, fluid cavity only
C: Chord of the swirl-slots
W/C: Pitch-to-Chord ratio

Figure 4. Geometry of labyrinth seal with swirl-brakes for Teeth-on-Rotor configuration

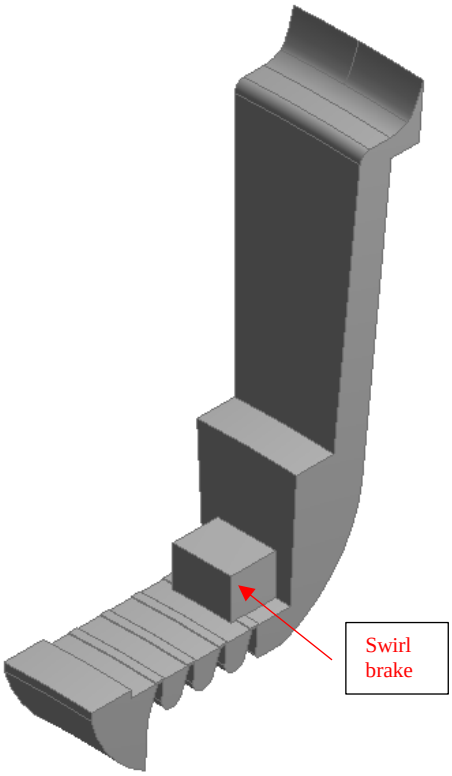

Figure 5. Shroud Cavity Flow Path with swirl-brake, Optimized Design

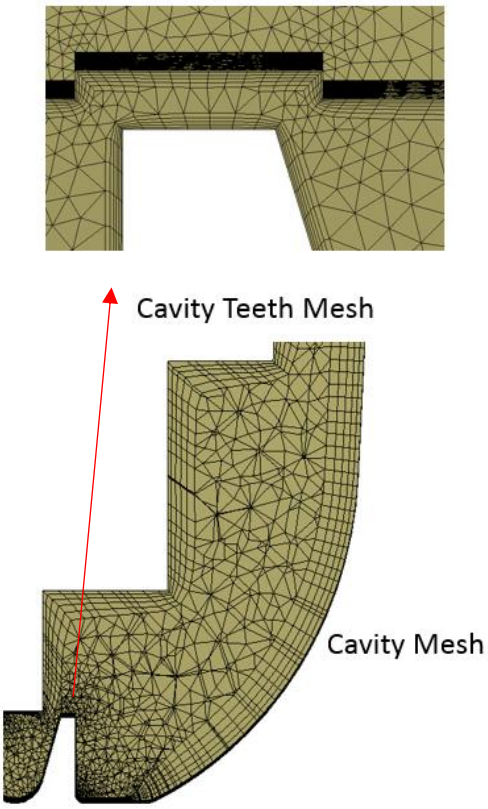

Figure 6. Shroud Cavity and Cavity-Teeth Mesh, swirl-brake Included, Optimized Design

In prior research, Moore et al. (2002) found that having between 30 and 90 swirl-brakes would give the maximum cavity swirl reduction. Based on the CFD optimization for the subject geometry, a total of 61 slots (vanes) was chosen. The choice of a large *prime* number was made to avoid any potential system resonance arising from blade passing frequency.

For a tooth-on-rotor design, the axial movement of the rotor is a critical factor in swirl-brake design. It was determined that the swirl-brake chord length be limited to 0.14 inches (3.56 mm). This ensures that, during operation, the rotor tooth would never move far enough axially to detract a second labyrinth tooth from sealing, thereby dropping the stage efficiency. The pitch to chord ratio is W/C=1.29, with the empty space encompassing two thirds of the circumference and the solid material including the rest (resulting in a 0.33 solidity ratio).

Table 2 lists a comparison of CFD-results between the baseline seal (without swirl-brakes) and the seal with swirl-brakes. Note the design with the swirl brake shows an increase in leakage of 10% through the cavity when compared to

the baseline design. While a small increase, this will lead to a drop in the overall stage and system efficiency. The table also shows that the inclusion of the swirl-brake does not appreciably increase the axial thrust load on the balance piston or the system power consumption.

Table 2. Comparison of CFD simulation - Baseline (no-swirl-brakes) seal and with swirl-brake design

Model	# of Swirl Slots	Slot Length (in)	Inlet Pressure P_{inlet} (psi)	Swirl velocity $Ct_{laby\ 1}$ (ft/s)	Swirl velocity $Ct_{average}$ (ft/s)	Laby1 Leakage (% flow)	Average Leakage (% flow)	Axial Force F_{axial} (lbf)	Power loss (hp)
No swirl-brakes	0	N/A	100	225	223	2.18	2.19	2,791	0.34
Swirl-brakes	61	0.14	100	-29	83	2.42	2.41	2,791	0.5

Ct: Circumferential velocity of the fluid
F_{axial}: Net Axial force on the stage (lb-f)
P_{inlet}: Pressure at stage inlet (psi)

Inclusion of the swirl-brake significantly reduced the average swirl velocity through the seal. Furthermore, it significantly reduced the swirl velocity at the first labyrinth tooth from the baseline case, to the extent it produced a negative pre-swirl. The slots (or vane-to-vane space) show generation of free vortices, leading to swirl reduction, as shown in Figure 7 below.

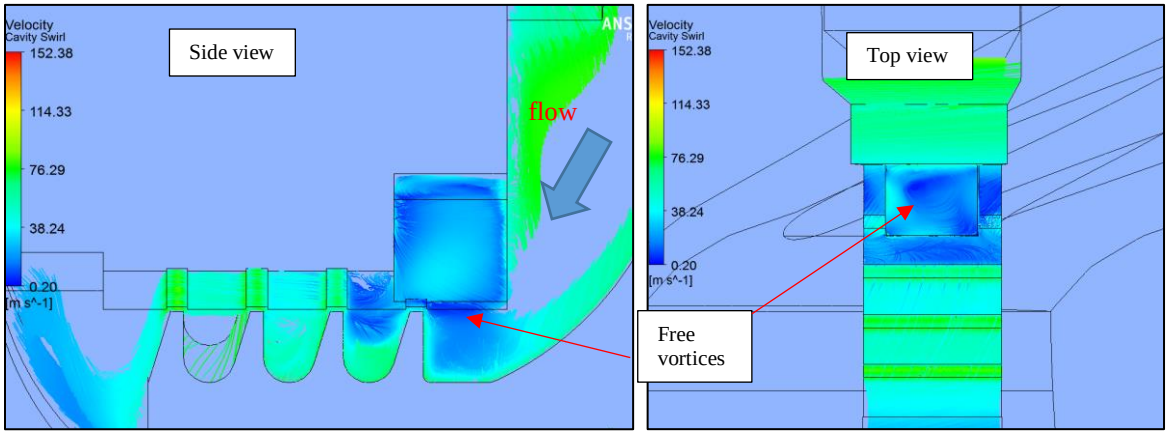

Figure 7. CFD stream-line plots showing generation of free-vortices within the swirl-brake.

Figure 8 shows the change in swirl velocity ratio at a cavity as a function of normalized axial distance. The normalized axial distance is taken from the cavity entrance at 0 (left of graph) and terminating at the cavity outlet at -0.99. The baseline swirl ratio → 0.6 towards the exit plane. However, the geometry including the swirl-brake shows a marked drop in cavity swirl ratio reaching a minimum of -0.06 at the region above the first labyrinth tooth. It is of note that the swirl-

brake has an effect that propagates upstream of the slot entrance. The cavity swirl increases within the labyrinth seal, but never reaches the baseline value.

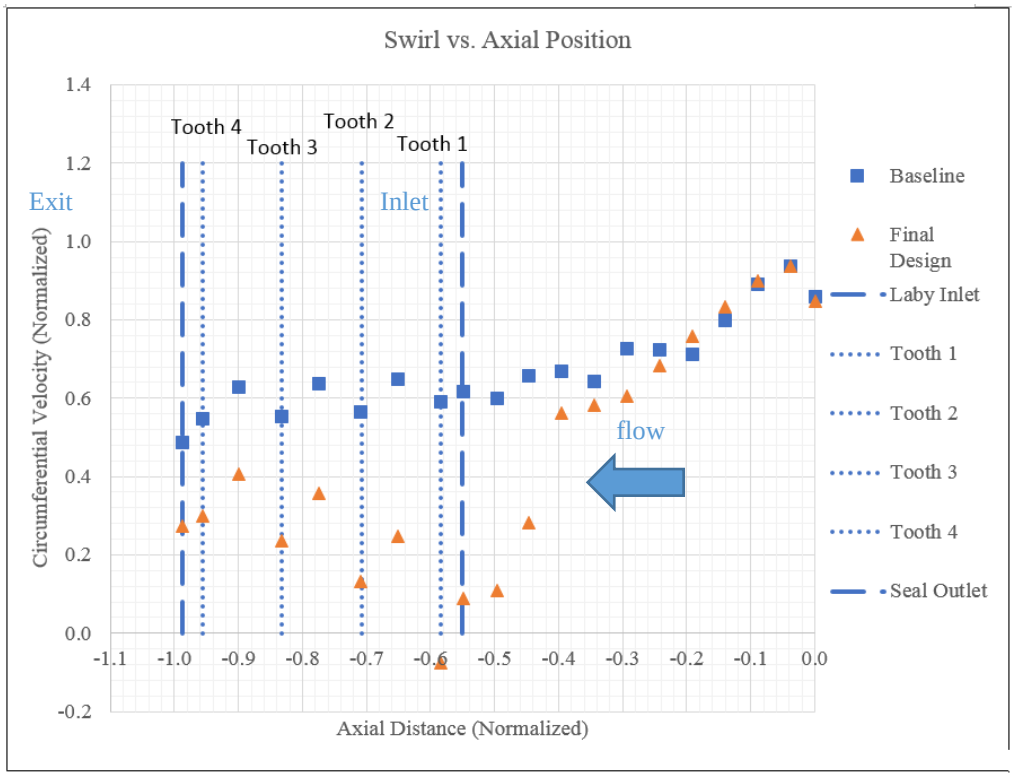

Figure 8. Comparison of Cavity Swirl Reduction - Baseline vs. swirl-brake design.

Figure 9 shows a comparison of the full shroud cavity swirl (circumferential) velocities, with and without swirl brakes. This shows the effectiveness of the swirl-brake particularly at the seal inlet. Table 3 lists the magnitude of the circumferential swirl velocities at a few key locations through the seal. Overall, the CFD simulation of the final swirl-brake geometry shows a significant decrease in the circumferential swirl at the seal inlet plane, thereby causing a lower average swirl through the seal cavities.

Table 3. Magnitude of the swirl (circumferential) velocities within labyrinth seal cavities

Location	Area-averaged Circumferential velocity, C_t **(ft/s)**	
	Baseline (Without Swirl-brakes)	With Swirl-brakes
Laby Inlet	234.7	33.7
Tooth 1	224.8	-29.3
Tooth 2	214.5	50.6
Tooth 3	210.7	89.2
Tooth 4	208.1	113.9
Laby Outlet	185.7	104.2
Average Across Seal	223.1	83.0

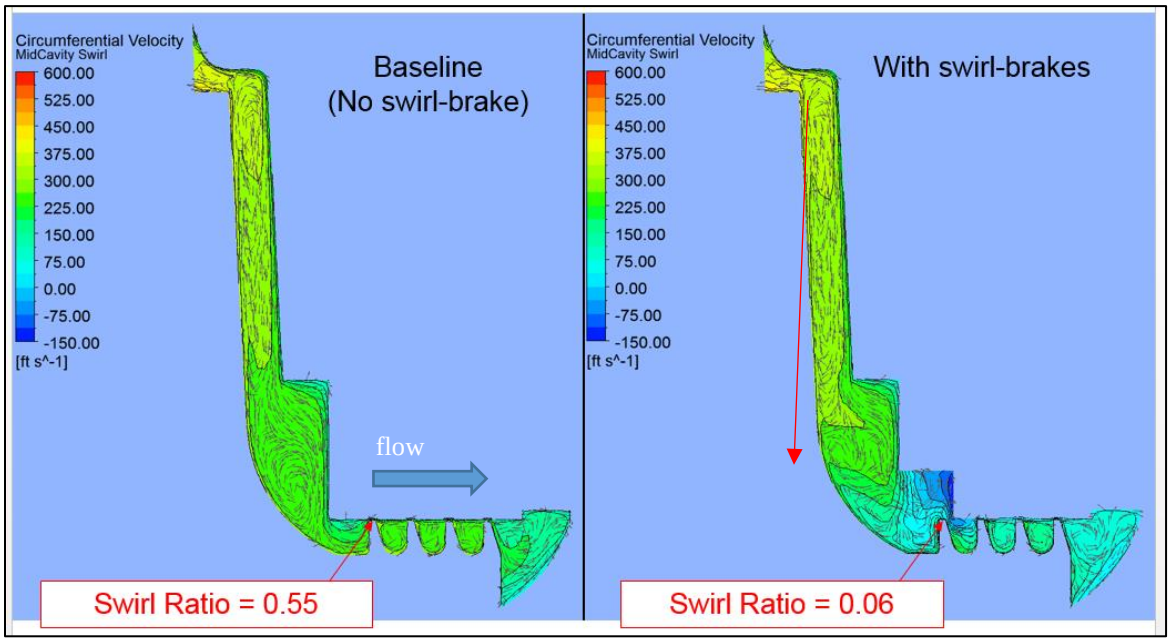

Figure 9. Comparison of cavity swirl-ratios as predicted by CFD, baseline and with swirl-brakes.

SUB-SCALE RIG-TESTING OF THE SWIRL BRAKES

A sub-scale testing of the swirl-brakes was performed at the facilities of one of the co-authors. The purpose of the testing was to determine whether a significant reduction in swirl velocity in the shroud cavity and downstream of the seal existed with the swirl-brake geometry and relative to the baseline design. The measurements would help to anchor the computational fluid dynamics (CFD) that could be used to further optimize the designs. In addition, the scaled-test results would help decide if full scale development testing of the swirl-brakes was warranted.

A Single Stage Test Rig (SSTR), rig capable of up to 22,000 rpm and 200 psi, was used for this purpose. The facility consists of an Open-Loop, 200 hp (at 3,600 rpm) electric motor with variable speed drive, a speed-increasing gearbox and a high-speed spindle rotor assembly. The test impeller is mounted to the spindle rotor assembly with a precision pilot fit and a tie bolt. Flow rate is measured at the inlet to the SSTR using a calibrated bell-mouth Venturi, and throttling takes place at the discharge via a control valve. The SSTR housing is insulated to minimize heat transfer to the environment.

Figure 10 shows the various features of the SSTR; the cross-section depicts a simple collector configuration for a representative performance test. The rig can accommodate various impeller and seal geometries by manufacturing the custom shroud side (and hub side if necessary) diffuser pieces.

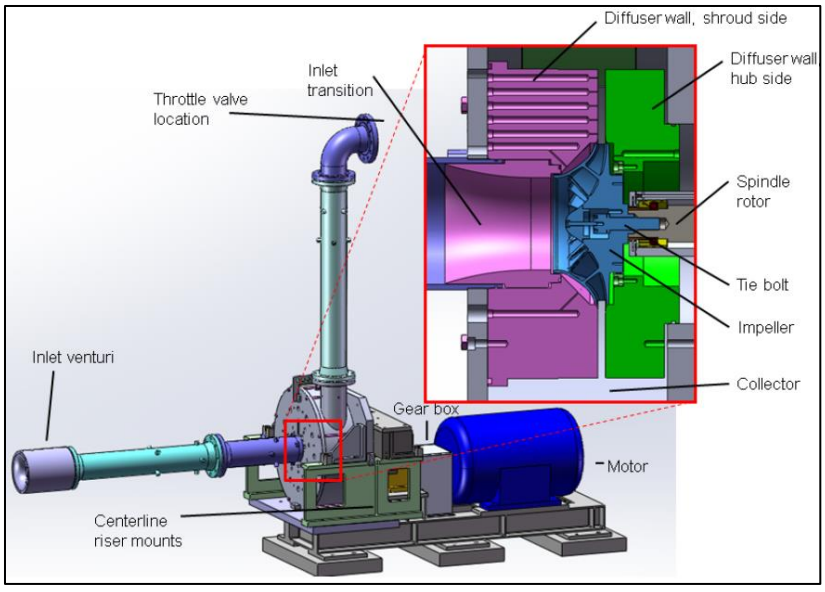

Figure 10. Single-stage Compressor test rig and the rotor-mount in the inset.

Pitot tube and static pressure measurements were added immediately upstream and downstream of the shroud seal to determine the circumferential velocity of the flow entering and exiting the seal, see Figure 11. The stator components in the rig were reworked to accommodate this instrumentation. A 0.032” set of Pitot tubes was used for upstream swirl

measurement and a 3-hole cobra probe was used for downstream measurement. Circumferential speed or swirl was measured at 2 different radial depths and 3 circumferential locations at 120° apart, upstream and downstream of the test seal.

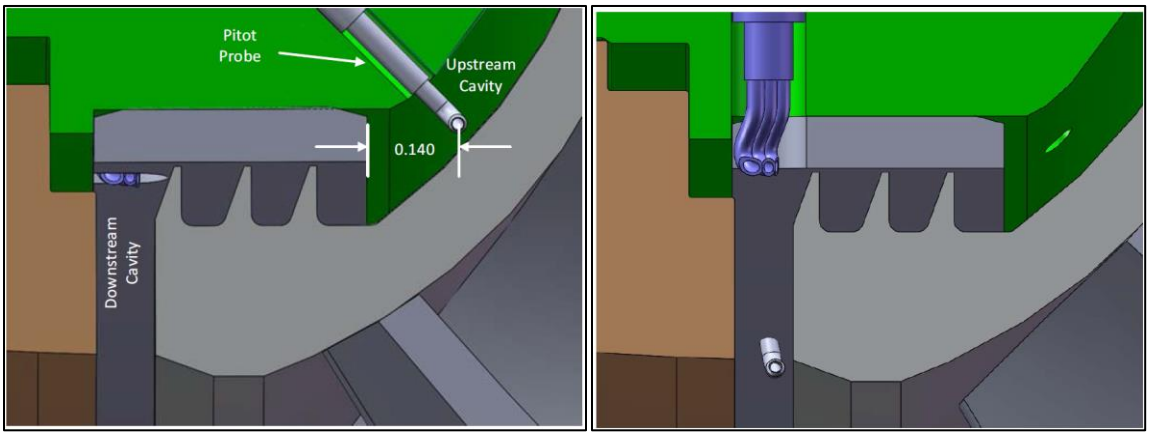

Figure 11. Location of Instrumentation to measure swirl in the single stage test rig

Note that the probes are extremely small, so positioning the probes repeatedly was very difficult; however, it was possible to achieve a depth accuracy of within approximately 4 mils of the target. This amounted to be approximately 3% of the shroud flow path width, which should be sufficient for the purposes of the test to capture the physical parameters.

Measuring swirl at the seal inlet was daunting. The instrumentation size had to be small enough to avoid impacting the flow through the cavity, yet rigid enough to measure reliably. Measurement was located just upstream of the seal inlet, as measurement right at the seal inlet is not possible.

Test data was collected for the swirl brakes with a similar impeller at 3 shaft speeds, 16,040 rpm, 19,240, 21,875 rpm. At each speed, the stage flow was throttled from choke to surge. At each flow, the pitot tube measurements were recorded for the calculation of the swirl. Measurements taken are shown in Figure 12 for both the baseline seal (left) and the swirl-brake design (right). Where the swirl is measured in the cavity, a 10-20% reduction in swirl velocities with the swirl- brakes is noticeable at the three operating speeds. Additionally, head flow characteristics were measured to determine the impact of the different designs on the aero performance of the compressor.

Table 4 lists the % reduction in swirl velocity with the swirl-brakes at two different measurement planes (upstream and downstream), and at two probe-immersion depths upstream. The shallow location did not show much change; however, the deep location upstream showed a 9% swirl reduction with swirl-brakes. Albeit small, the measurement matched well with CFD predictions for the same location upstream of the seal inlet. It gave the confidence that further reduction of swirl was possible closer to seal inlet, though not measurable due to the constraints mentioned earlier. Also, the downstream measurement showed a 15% decrease in swirl.

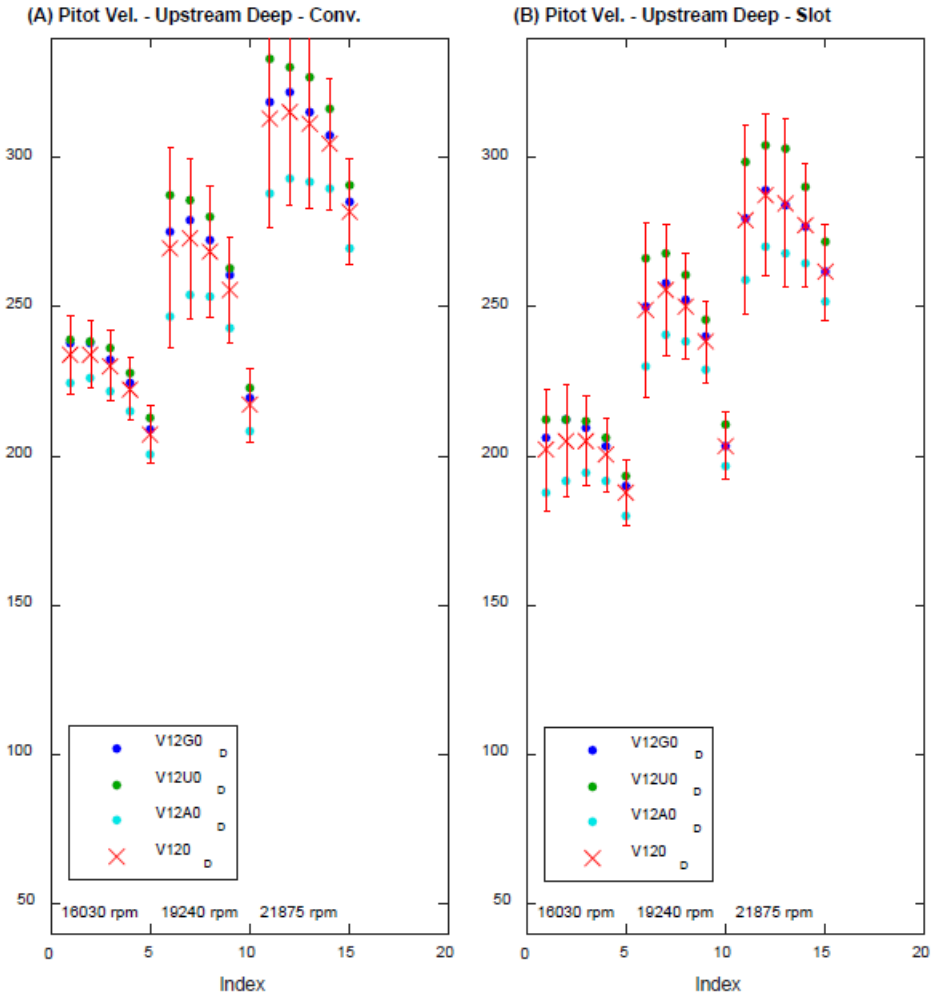

(a) Seal with no swirl brake (b) Seal with swirl brake

Figure 12. Measured swirl velocities (Pitot tube) upstream of seal inlet. Left : baseline seal and Right: Seal with swirl-brake.

Tip Speeds @ seal inlet = 456 ft/s (139 m/s), 16030 rpm; 548 ft/s (167 m/s), 19240 rpm; 623 ft/s (190 m/s), 21875 rpm

V12G0 (80°) , V12U0 (260°) and V12A0 (350°) are pitot velocities measured at 3 circumferential Deep locations, upstream of seal inlet. V120 is the circumferentially averaged values.

Table 4. Scaled-rig swirl-brake test results: baseline vs. swirl-brakes

Location	% reduction in inlet swirl	
	Measured	CFD Predictions
Upstream Deep (close to impeller surface)	9.0	6.2
Upstream Shallow (close to shroud surface)	-0.2	0.8
Downstream	15.6	9.8

Thus, the scaled-rig testing definitively indicated that the swirl brake designs have a major impact on swirl velocities relative to the baseline design. Based on this, the pace of full-scale testing was accelerated. The testing successfully utilized the rig to provide performance and detailed pressure, velocity measurement data for the swirl-brake designs.

FULL-SCALE CLOSED LOOP TESTING

An integral part of the swirl-brake development was extensive full-scale development testing at a closed-loop facility at operating conditions far beyond typical sales applications for this compressor. The closed-loop facility has 12" (305 mm) piping with ANSI 900# flanges, capable of reaching up to 2250 psia (155 bar) flange rating with Nitrogen as the working gas.

A six-stage rotor was selected for studying the effect of swirl-brakes. The compressor was tested multiple times, with and without swirl-brakes, at equivalent site conditions. While swirl-brakes were added to all six impeller shroud seals, the hub seals were left intact without swirl brakes. Aerodynamic performance was recorded with instrumentation and standards meeting the ASME PTC10 Type II requirements. Rotor radial (and axial) vibration was monitored through proximity probes located near the journal bearings. The excitation of the resonant sub-synchronous vibrations was monitored through spectral analysis of the proximity probe output and this was the primary determinant in assessing the stability improvement. It would have been ideal to use an external frequency-dependent excitation (like a magnetic-exciter) on the rotor or non-intrusive techniques such as Operational Modal Analysis (OMA) to quantify the stability improvement, but geometric constraints ruled out their use on these tests. The OMA technique and its implementation in determining rotordynamic stability of a compressor rotor is shown by Baldassarre et al (2015).

Figure 13 shows the vibration characteristics of the rotor at the rated condition in two different tests. On the left, the waterfall plot obtained while testing the rotor without swirl-brakes shows the excitation of the first resonance frequency at ~ 145 Hz. The peak-to-peak amplitude levels at the resonant condition are bound, however this would still be detrimental to the reliable operation of a compressor if this were to show-up at site operation. On the right of Figure 13, the same rotor tested with swirl-brakes on the shroud-seals of all 6 stages shows no excitation of the resonant frequency. These tests were repeated thrice, with the compressor and rotor disassembled and reassembled each time, to verify repeatability and consistency. To keep out the uncertainties from bearing tolerances when evaluating the swirl-brakes, the same identical bearing was used to test the rotor. In addition to the above-mentioned tests, some tests were repeated with a new, different bearing in order to study the sensitivity of bearing tolerances to rotor stability characteristics.

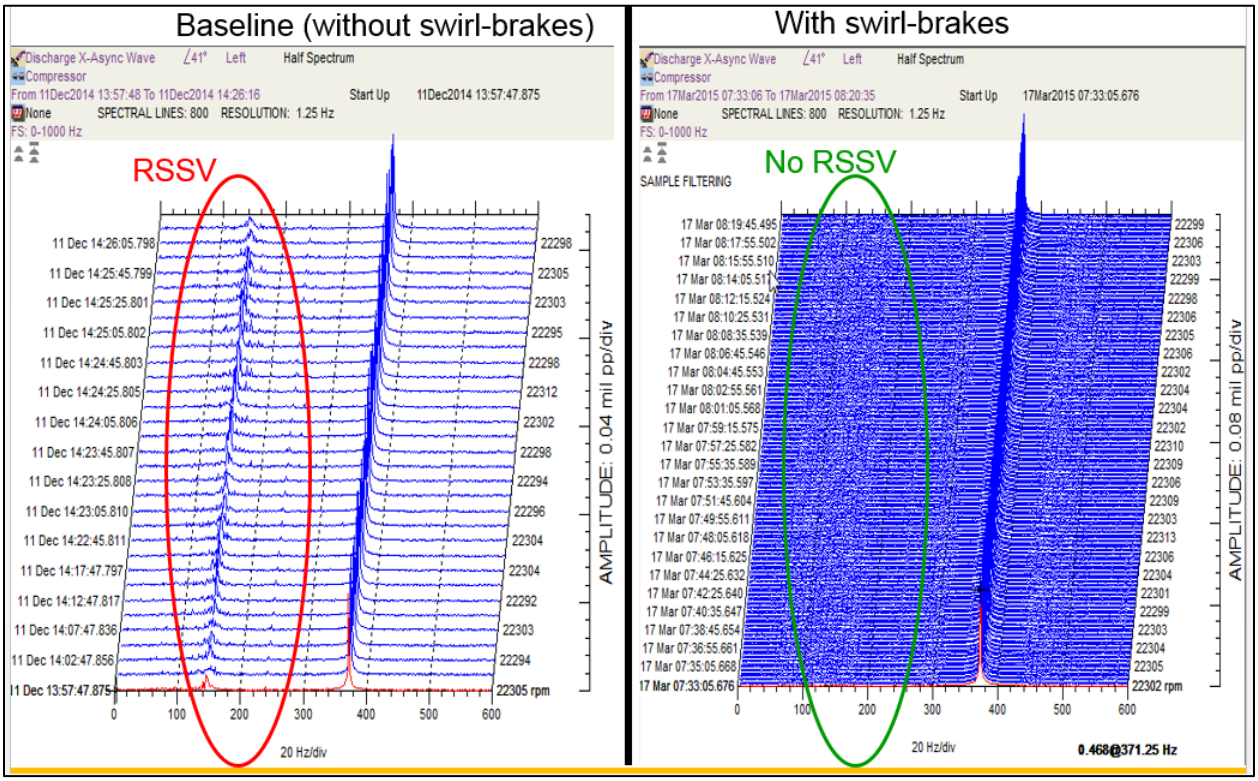

(a) Rotor with stage seals with no swirl brakes (b) Rotor with seals with swirl brakes

Figure 13. Full-scale shop testing results at rated conditions – without Swirl-brakes (presence of sub-synchronous vibrations) and with Swirl-brakes (no signs of sub-synchronous vibrations).

The rated condition and other conditions at which the performance of swirl-brakes were confirmed are plotted on the API chart for reference in Figure 14 (without swirl-brakes) and Figure 15 (with swirl-brakes). The Red indicates presence of resonant sub-synchronous vibrations (RSSV) and Green indicates absence of RSSV, at the corresponding operating conditions. As shown, sub-synchronous vibrations are always excited for the rotor without swirl-brakes, albeit at different levels for the various test conditions. By comparison, the rotor with swirl-brakes at identical conditions does not show any sub-synchronous vibrations.

The aerodynamic performance of the compressor measured with and without swirl brakes showed a very minimal impact from the swirl brakes. With the swirl brakes on the shroud seals of all 6 stages, the overall compressor efficiency dropped less than 0.7%. This is a negligible impact on the isentropic head.

Based on the successful outcome, the swirl-brake designs were qualified for field installation.

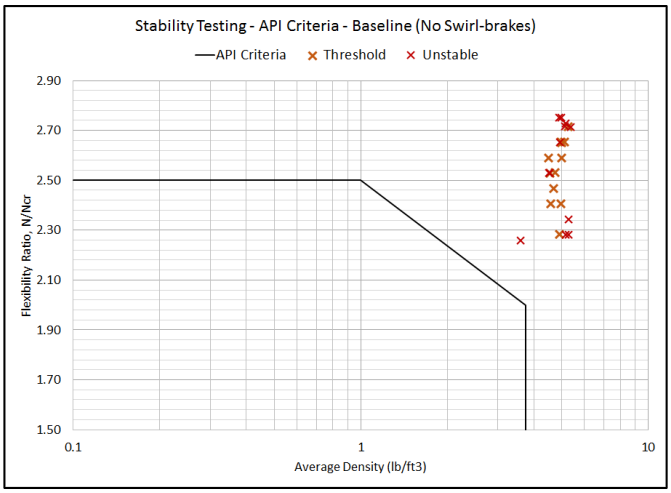

Figure 14. Test data with the Baseline rotor (no swirl-brakes) on the API stability chart

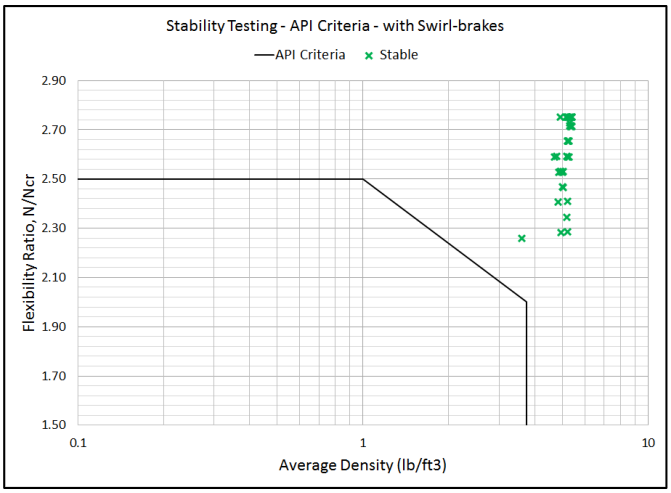

Figure 15. Test data of the rotor with swirl-brakes on the API stability chart

COMPARISONS BETWEEN TEST DATA AND ROTOR SIMULATION

A rotordynamic analysis was conducted on the rotor with and without swirl-brakes and compared to the full-scale test data. A Finite-Element code developed in-house at the OEM was used to model the rotor-bearing system. The rotor model had been calibrated with modal testing. The first three free-free (undamped) modes measured during modal testing were matched with the simulation results to within 1.3%.

The bearing analysis was performed using a commercial bearing code. The combined rotor-bearing model has been calibrated with data from many years of testing at the OEM facility to the measured damped critical speeds. The primary impact of the swirl-brakes in modeling arises in the swirl-ratio parameter used to calculate the seal dynamic force coefficients. The stability analysis incorporated a swirl-ratio of 0.55 (at seal inlet) for the baseline case and a swirl-ratio of 0.1 for the case with swirl-brakes. Comparison was made on the basis of the API Level I and Level II calculations. The swirl-ratio upstream of the Balance Piston seal, which has a shunt-injection, was assumed to be 0.2. A commercial labyrinth seal code was used to predict seal force coefficients.

Table 5 lists the operating conditions at which the rotordynamic simulation was performed. This particular case was chosen since this was one of the main conditions at which the compressor was tested with and without swirl-brakes.

Table 5. Operating conditions for rotordynamic simulation

Parameters	Details	
Inlet Pressure	600 psig	41.2 bar
Exit Pressure	2160 psig	148.5 bar
Inlet Temperature	90 F	32.2 °C
Exit Temperature	355 F	179.4 °C
Test gas	Nitrogen	

A stability analysis, Level I and II as recommended by API 617, was performed on the rotor-bearing system. Results are presented for the Level II analysis due to the inclusion of seal coefficients. Table 6 shows the logarithmic decrement (log dec) as predicted by the simulation, with and without the swirl-brakes, and for the minimum, nominal, and maximum bearing clearances.

Whereas the case without the swirl-brakes show the rotor to be marginally stable (~0.07) at the extreme operating conditions tested, the case with the swirl-brakes shows a significant increase in logarithmic-decrement, due to lower cross-coupling stiffness predicted. The quantitative improvement in the stability threshold seen in the rotordynamic simulation with swirl-brakes matches very well with the qualitative improvement seen during the testing.

Table 6. Comparison of logarithmic decrements with and without swirl-brakes based on simulation

Logarithmic Decrement from simulation	Minimum Bearing Clearance	Nominal Bearing Clearance	Maximum Bearing Clearance
W/o Swirl-brakes (baseline)	0.07	0.15	0.24
With Swirl-brakes	0.40	0.56	0.70

FIELD EVALUATION AT AN OFF-SHORE INSTALLATION

Having qualified the swirl-brake design with scaled-rig testing and full-scale pressurized loop testing, the OEM waited for evaluating the long-term full-load performance of the swirl-brakes at a suitable field installation. That opportunity came in 2015.

An end-user had employed the subject compressor model at an off-shore installation for gas reinjection. After having successfully operated their existing compressor for over 16 years, the end-user approached the OEM with requests for restage, overhaul and suitability-review to operate at more stringent operating conditions – beyond the stability threshold of the compressor's standard design. The concerns with the compressor stability at the newly proposed conditions were shared with the end-user, and they were also provided with the option of either using the recently-developed swirl-brakes or a fully-qualified existing design of a squeeze film damper. A design audit was conducted with the end-user's Rotating Equipment team and the site Project team. The end-user chose the swirl-brake design for their application.

The compressor was sent to the OEM's Overhaul facility in Texas. At assembly of the restaged compressor, the labyrinth seals with milled swirl brakes were installed at each impeller shroud-seal location, in lieu of the standard seals that had no swirl-brakes. The restaged compressor had 7 stages.

The compressor with swirl-brakes was re-commissioned at the off-shore installation in early 2016, and has been running successfully since then. Results confirm stable operation in the field with swirl-brakes. A recent snapshot of the compressor's site performance was obtained through the OEM's remote monitoring system, and is provided with the end-user's permission, see Figure 16. The compressor has been operating successfully at site for over a year now at discharge pressures between 1300 to 1900 psig. The unit is operating at maximum speed, with vibration well below 1.0 mil peak-to-peak, at all operating pressures.

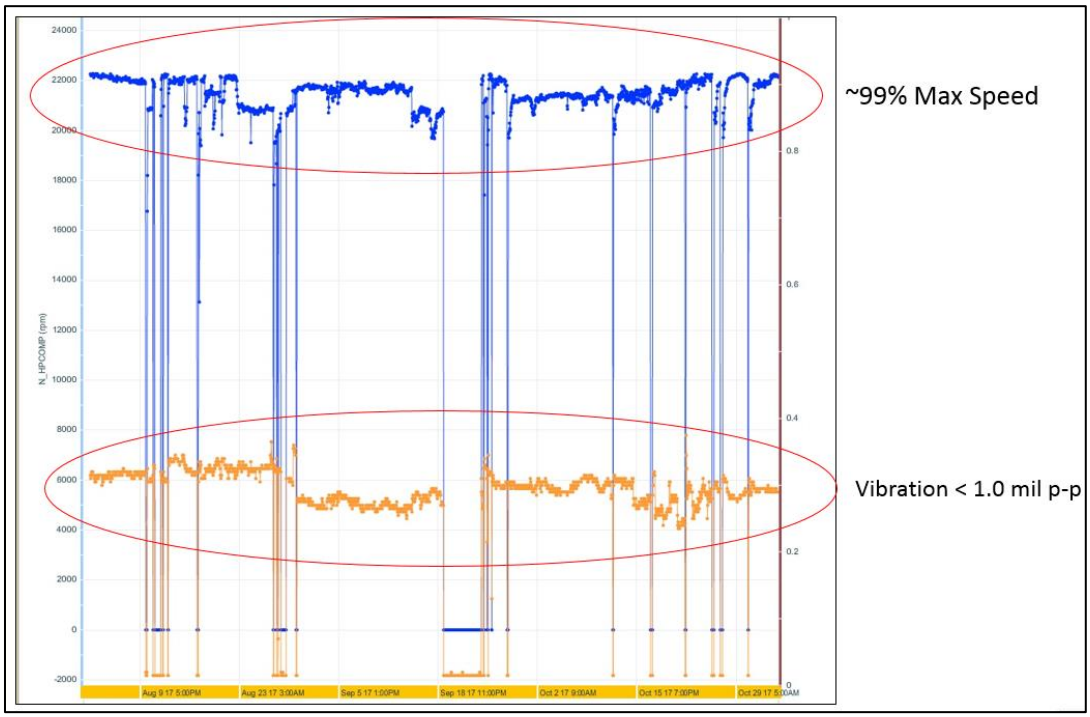

Figure 16. Compressor at site modified with swirl brake seals: rotor peed and vibration trend data over 4 months of operation.

CONCLUSION

Swirl-brakes have been used successfully in high-pressure pump and compressor applications for many years. This paper presents the design and implementation of swirl brakes for a centrifugal compressor family with Teeth-on-Rotor seal configuration. Discussion includes:

a) Aerodynamic design of swirl brakes with the help of Computational Fluid Dynamics (CFD). The use of swirl-brakes showed a 90% reduction of the swirl ratio at seal inlet.

b) Sub-scale testing of the swirl-brake design in an instrumented single-stage test rig to measure the inlet swirl ratio in shrouded impellers. This confirmed the CFD predictions.

c) Full-scale prototype shop-testing and qualification (with and without the swirl-brakes) was performed in a closed-loop test facility. It demonstrated the stability improvements with the swirl-brakes. Incorporating the swirl-brakes enabled the compressor to avoid any signs of rotordynamic instability at certain extreme conditions where the compressor showed significant RSSV without the swirl-brakes.

d) Comparison to numerical predictions of a rotordynamic model, which confirmed a significant improvement in the logarithmic decrement of the rotor-bearing system with the swirl-brakes.

e) Successful operation of an off-shore compressor installation with swirl-brakes.

In summary, the knowledge contributions of this paper to the archival literature are:

- Implementation of swirl brakes for abradable-Tooth-on-Rotor seal designs for compressors
- Laboratory testing of scaled swirl-brake designs to measure swirl ratios upstream of the seals and correlation to CFD predictions
- Successful implementation of the swirl brake design to an off-shore installation to improve rotor-dynamic stability.

ACKNOWLEDGEMENTS

The authors thank the Shell Company and Solar Turbines for agreeing to publish the data. In addition, the contributions of Marco Vagani, Anand Srinivasan and Ricardo Torres during the design, manufacturing and testing of these compressors are gratefully acknowledged. The commercially available ANSYS-CFX Workbench software, THPad® (University of Virginia), and XLLaby® (Texas A&M University) were employed in this project.

REFERENCES

Benckert H., and Wachter J., 1980, “Flow Induced Spring Coefficients of Labyrinth Seals for Application in Rotor Dynamics”, Proceedings NASA Lewis Research Center Rotordynamics Instability Problems in High-Performance Turbomachinery, pp. 189-212.

Sivo, J.M., Acosta, A.J., Brennen, and C. E., Caughey, T.K., 1995, “Influence of Swirl Brakes on the Rotordynamic Forces Generated by Discharge-To-Suction Leakage Flows in Centrifugal Pumps, “ Journal of Fluids Engineering, 117, pp. 104-108.

Baumann, U., 1999, “Rotordynamic Stability Tests on High-Pressure Radial Compressors” Proceedings of the 28th Turbomachinery Symposium, Turbomachinery Laboratory, Texas A&M University, College Station, Texas, pp. 115-122.

Fozi, A.A., 1986, “An Examination of Gas Compressor Stability and Rotating Stall,” Rotordynamic Instability Problems in High Performance Turbomachinery, NASA CP2443, Proceedings of a Workshop held at Texas A&M University, pp-445-459.

Moore, J. and Walker, S., and Kuzdzal, M., 2002, "Rotordynamic Stability Measurement during Full-Load, Full-Pressure Testing of a 6000-psi Reinjection Centrifugal Compressor", Proceedings of the 31st Turbomachinery Symposium.

Childs, D. W., 1993, *Turbomachinery Rotordynamics,* John Wiley & Sons, New York, New York.

Moore, J.J., and Palazzolo, A.B., 1999, "Rotordynamic Force Prediction of Whirling Centrifugal Impeller Shroud Passages Using Computational Fluid Dynamic Techniques," ASME Paper No 99-GT- 334.

Nielsen, K.K., Myllerup, C.M., and Van den Braembussche, R. A., 1998, "Optimization of Swirl Brakes by Means of a 3D Navier-Stokes Solver, ASME Paper 98-GT-328.

Moore, J. and Hill, D., 2000, "Design of Swirl Brake for High Pressure Centrifugal Compressors using CFD Techniques", International Symposium on Transport Phenomena and Dynamics of Rotating Machinery, Honolulu, Hawaii.

Baldassarre, L., Bernocchi, A., Fontana, M., Guglielmo, A., and Masi, G., 2014, "Optimization of Swirl Brake Design and Assessment of its Stabilizing Effect on Compressor Rotordynamic Performance", Proceedings of the 43rd Turbomachinery Symposium, Turbomachinery Laboratory, Texas A&M University, College Station, Texas.

Untaroiu, A., Heyrapetian, V., Untaroiu, C., Wood, H., Schiavello, B., and McGuire, J., 2013, "On the Dynamic Properties of Pump Liquid Seals", Journal of Fluids Engineering, 051104-1.

Pugachev, A.O., and Deckner, M., 2012, "Experimental and theoretical rotordynamic stiffness coefficients for a three-stage brush seal", MSSP, 31, pp. 143-154.

Baldassarre, L., Guglielmo, A., Catanzaro, M., Zague, L., Silva, R., Ishimoto, L., and Miranda, M., 2015, "Operational Modal Analysis Application for the Measure of Logarithmic Decrement in Centrifugal Compressor", Proceedings of the 44th Turbomachinery Symposium, Turbomachinery Laboratory, Texas A&M University, College Station, Texas.

API 617, 2002, "Axial and Centrifugal Compressors and Expander-Compressors for Petroleum, Chemical and Gas Industry Services", 7th Edition, American Petroleum Institute, Washington, D.C.

API 684, 2005, "API Standard Paragraphs Rotordynamic Tutorial: Lateral Critical Speeds, Unbalance Response, Stability, Train Torsionals, and Rotor Balancing", 2nd Edition, American Petroleum Institute, Washington, D.C.